

EXPERIMENTAL AND COMPUTATIONAL INVESTIGATION IN THE RESONANT VIBRATION OF 3D-PRINTED PLA THIN RECTANGULAR PLATES

M. Dutczak*, J. Shelton*[†]

*Department of Mechanical Engineering, Northern Illinois University, DeKalb, IL 60115

[†]Corresponding Author Email: jshelton4@niu.edu

Abstract

When a plate is vibrated at the frequency of a resonant normal mode, the plate exhibits a 2D standing wave pattern with characteristics determined by its geometry, material properties, and boundary conditions. A visualization of these vibrational patterns is popularly called Chladni patterns and is named after late 18th century German scientist Ernst Chladni. As designers and engineers continue to explore innovative applications for 3D printed materials, it is important to ensure that these fabricated parts possess mechanical resonant frequencies that match those fabricated from traditional processes. As an acknowledgement of a long-standing history here at Northern Illinois University in the study of vibrating elastic plates through the work of Professor Thomas Rossing, the objective of this investigation is to determine the relationship between 3D printing layer height and vibrational response for fused deposition modeled (FDM), polylactic acid (PLA), 3D-printed, thin rectangular plates. Experimental and computational analyses are performed to describe the free vibration of centrally clamped plates with free edge boundary conditions on all four sides indicated (FFFF). In the experimental analyses, 100% infilled specimens of five different 3D printed layer heights were fabricated and driven via a mechanical wave driver across the frequency range of 1-4000 Hz. Experimental visualizations of the standing wave patterns were performed using sand. The relationship between layer height and vibrational response for nine mode shapes was found. In the computational analysis, finite element modal analysis was used on thin rectangular plates possessing standard PLA material properties. It is concluded in this study that by decreasing the fabrication layer height to the minimum layer thickness of 0.05 mm, the experimentally observed resonant frequency for a given mode shape in the 3D printed rectangular plate approaches an approximately 3% deviation from the values calculated by finite element analysis. It is believed that as the layer height decreases, the number of connections in the plates increases, resulting in the increase of homogenous tendencies within the plate body.

Keywords: PLA, 3D-printing, Mode shapes

Introduction

Advances in the 3D printing of PLA-based parts continue to strive to meet the engineering demands of both rapid prototype and production-level parts. This has led to interest in the development of an understanding of the various static and dynamic mechanical properties and characteristics of these 3D-printed PLA parts. Most 3D printing-based investigations have focused on how static mechanical properties, such as elastic modulus, yield stress, ultimate tensile stress, and hardness, are affected by the parameters specified at the outset of the 3D printing process. For example, El Fazani et al. looked at how infill density affects the ultimate tensile strength, yield

stress, and elongation of tensile test coupons [1]. In their investigation, parts that were fabricated with 100% infill were found to yield the highest tensile strength, with a value of 48 MPa. The conclusion drawn from their results suggests that the voids created by the lower infill percentages contributed to decreases in tensile strength characteristics of the 3D printed parts. Frunzaverde et al. studied the influence of layer height on the tensile strength of FDM-Printed PLA specimens [2]. In their investigation, it was concluded that the tensile strength in the specimens tested decreased 23.41% as the layer height increased from 0.05 mm to 0.2 mm. Stojkovic et al. also performed an experimental study on the impact of layer height on tensile strength of FDM 3D-printed parts of various materials [3]. In this investigation, the PLA specimens fabricated at layer heights of 0.1 mm, 0.2 mm, and 0.3 mm resulted in decreases in tensile strength, with values of 32 MPa, 30.19 MPa, and 28.75 MPa, respectively.

The numbers of investigations that involve determining the dynamic mechanical characteristics of 3D printed PLA-based parts are considerably less than the number of investigations focused on the static mechanical characteristics, as discussed above. However, Nguyen, et al. stresses that an understanding of these dynamic mechanical characteristics is equally as important as their static counterparts, since they ensure the reliability and structural integrity of 3D printed components under dynamic loading conditions [4]. The experimental investigations that have focused on the dynamic mechanical characteristics of 3D printed parts have focused on how their modal characteristics are affected the parameters specified at the outset of the 3D printing process. For example, Nguyen, et al. performed experimental modal analysis of additively manufactured polymers under dynamic loading conditions while varying part adhesion to the print bed, print direction, and layer thickness [4]. Results from this study indicate that adhesion type to the print bed had the most significant effect on the dynamic moduli, natural frequencies, and damping coefficients compared to the other 3D printing parameters. He et al. investigated the effect of infill pattern, infill density, and nozzle size on the damping ratio and loss factor of parts fabricated using FDM [5]. This investigation observed that among the 3D printing parameters investigated, infill density had the most significant effect on the damping ratio, with higher infill densities resulted in lower damping ratios. Medel et al. [6] investigated the relationship between stiffness and damping behavior of 3D printed specimens. In the study, the interface between filaments was judged the key factor in damping behavior, with lower damping ratios indicating superior interfilamentous bonding. While layer thickness did not affect damping performance in this study, its influence cannot be completely ruled out, as layer height levels not included in this study (≥ 0.3 mm) might decrease interfilamentous bonding.

In this investigation, a continued understanding of effects of 3D printing process parameters on the modal characteristics of 3D printed rectangular plates is developed and presented. While a similar analysis was performed by Abdeddine et al. [7], the effects of 3D printing process parameters were not investigated. In a manner that follows the long-standing history established by Professor Thomas Rossing here at Northern Illinois University [8], [9], this investigation will adapt his established methodological approach in studying the sensitivities of resonant frequencies to the layer height of the 3D printed rectangular plate. These experimental results are compared to those obtained from finite element analyses.

Design and Methodology

3D printing fabrication of rectangular plate

The plate specimens used for this study were designed in SolidWorks 2023 (Dassault Systèmes) using metallic Chladni plates as a reference. The 3D-printed plates dimensions were 152.4 mm × 152.4 mm × 1.5875 mm in XYZ direction, respectively (see figure 1). The plate was designed with a centrally located connection point to the vibration generator.

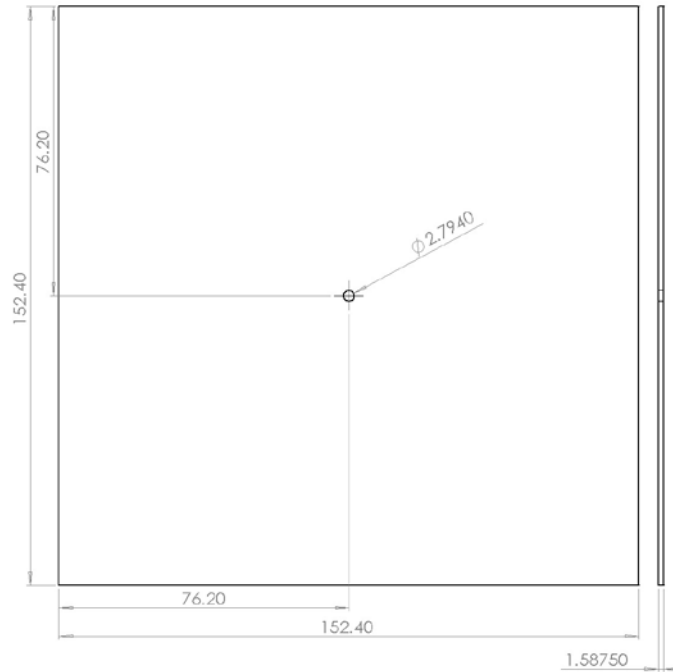


Figure 1. Schematic of 3D-printed plate with dimensions included (in millimeters).

The designed test specimens were then sliced into G-code using the slicer software PrusaSlicer 2.7.2 (Prusa Research, Czech Republic). The slicer software allows for control of several 3D printing process parameters, including layer height, infill percentage, infill style, printing speed, nozzle temperature, bed temperature, and the feed rate of the material. The parameters chosen for the test specimens in this study are presented in table 1.

Table 1. Parameters used during 3D printing fabrication process of rectangular plates.

Nozzle Temperature (°C)	215
Bed Temperature (°C)	60
Layer Thickness (mm)	0.05,0.10,0.15,0.20,0.25
Infill Percentage (%)	100
Infill Style	Rectilinear
Raster angle	45°
Printing Speed (mm/s)	
- Perimeters	40
- Infill	80
- Top Solid Infill	40
Feed Rate (mm ³ /s)	15

All test specimens were fabricated by a Prusa Mini FDM 3D-printer with a 0.4 mm nozzle. Each specimen was fabricated from a single spool of Elegoo PLA filament having a diameter of $1.75\text{mm} \pm 0.02\text{mm}$. The filament was heated to 215°C and extruded onto a heated printing bed at 60°C for improved adhesion. Each bead of material is deposited onto the print bed in a form assumed to have a cross section similar to that presented in figure 2 (left). Figure 2 (right, top) shows two tangent beads of material deposited in such a way to cause a void between them. In order to get the desired 100% infill, the slicer program overlaps the beads to fill the space and bond the beads together (see figure 2, right, bottom). The infill style is defined by a multidirectional texture where the direction of deposition is different between layers to achieve a more isotropic mechanical response for the 3D-printed part. This follows a similar approach performed by Song et al. which resulted in an elastic response of the 3D-printed PLA part being approximately isotropic [10].

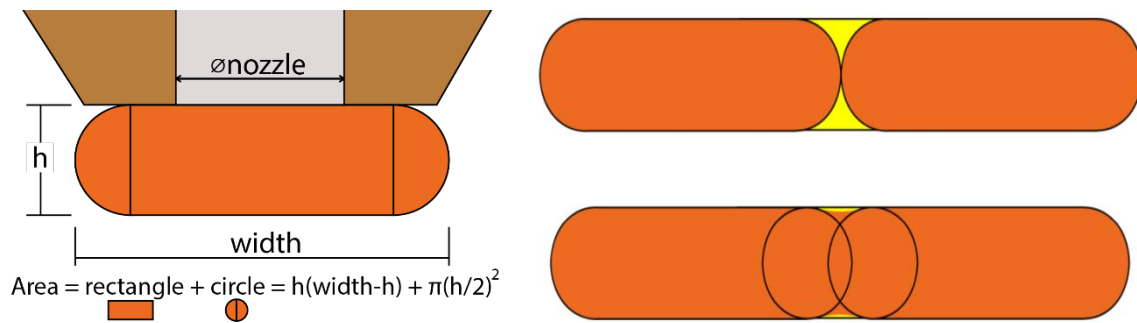


Figure 2. On the left, the dimensions of the deposited 3D printed material is presented. On the right, a schematic of how material is deposited to minimize voids during the 3D printing process [11].

Experimental setup

The experimental platform used in this investigation is shown in figure 3. An electromechanical wave driver (Arbor Scientific P7-1000) drove each 3D printed thin plate. Each plate was fixed to the electromechanical wave driver by a M6 6 mm screw located at the center point. The wave driver has a frequency range of 1-4000 Hz with a 1 Hz accuracy from 0 – 400 Hz and a 10 Hz accuracy from 400 – 4000 Hz. The mechanical wave driver interfaced directly to a Hewlett Packard 33120A waveform generator. The chosen peak-to-peak voltage was 20 V_{pp}, the

max output of the waveform generator. The mechanical wave driver has a current limit of 1 A. The Generator has 50Ω of built-in resistance, resulting in 0.4 A through the wave driver.

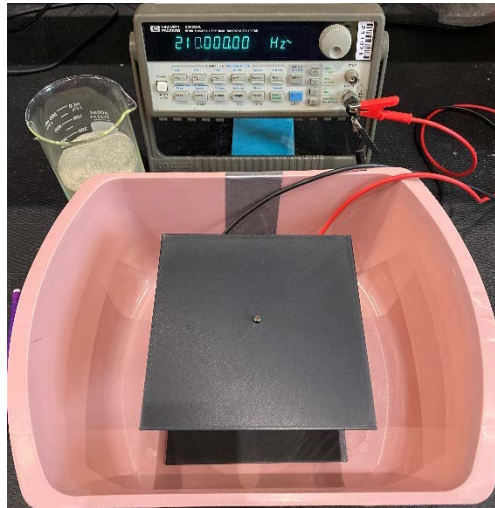


Figure 3. Experimental setup used in this investigation.

Sand is used for visualizing the patterns formed for each vibrational mode of the 3D-printed thin plate. Sand particles were spread uniformly on the 3D printed thin plate and then the frequencies of the mechanical wave driver were changed until a stable pattern was formed. For each mode analyzed, a range of frequencies was found to excite the 3D-printed thin plate. Throughout the range of excitation, the plates vibrational response increased and decreased around the experimentally determined frequency. The range for each mode shape was incrementally iterated through with auditory and observatory factors. As the plate approached the frequency of highest response an auditory sound was produced. This sound varied depending on the vibrational mode that was being approached. The frequency which produced the loudest auditory response helped indicate the frequency of highest response. Along with the auditory indicator a physical observational indicator of watching the excitation response of the sand on the plate was considered, Incremental tests were taken to determine the frequency with highest response with these two indicators. After each test and pattern found, a reset of sand on the plate was performed to ensure sand was uniformly spread on the plate for each mode shape and that the pattern found is repeatable. Once a stable pattern of sand was formed on the plate, a picture of the pattern was taken with a camera. This process was repeated five times to obtain a statistical average. Experimentation of all plates were tested on the same day in the same experimental setup for accuracy in testing procedure.

Finite element model setup

A corresponding finite element analysis was also performed to provide numerical simulation results as a comparison to the results obtained from the experimental setup. The ANSYS Workbench version 2023 software package was used to generate the mode shapes results of similarly formed thin plates. In the simulation environment of ANSYS Workbench, the thin plate geometry is a square with a side length of 152.4 mm and a thickness of 1.5875 mm. The

mesh for this computational study includes 22,979 elements, with an element size of 2.5 mm, and 46,709 nodes for the plate. The mesh of the geometry is shown in figure 4.

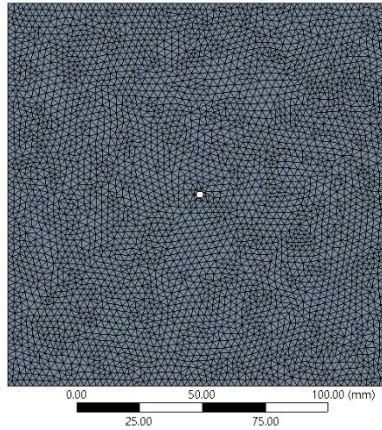


Figure 4. Computational Mesh used for ANSYS simulations.

The plate geometry was modeled with a material classification of PLA using the material properties provided by the software. These material properties of PLA are shown in table 2 below. PLA has a Poisson’s ratio of 0.35. The setup of the analysis in ANSYS included for the system a displacement boundary condition at the central hole for attachment to the vibration generator. This displacement was fixed in the x , and z directions and free in the y direction. Fixed support boundary conditions at the top and bottom edge of the connection hole were implemented as the plate is clamped between the top and bottom of the connection point to the vibration generator. The built-in modal analysis module within ANSYS was used.

Table 2. The materials properties of PLA used in the ANSYS simulations.

Density (kg/m ³)	1250
Tensile Yield Strength (MPa)	54.1
Tensile Ultimate strength (MPa)	59.2
Poisson Ratio	0.35

Results and Discussion

Computational Results

In figure 5, the mode shapes and the associated modal frequencies generated from finite element analysis of a thin square PLA plate with free boundary conditions on all side edges is presented. The hotter color map colors indicate the antinodes of the resonant frequency and the colder color map colors indicate the nodes in which the sand will gravitate to and settle on. Jiao et al. [12] calculated similar mode shapes of a square plate made of silicon for our modes 1, 2, 3, 4 and 5 from their finite element analyses. However, there was one mode shape that was not observed in our investigation that would have appeared before our mode 1. This is perhaps due to the material properties and simulation parameters, since the associated model frequencies determined by their finite element analysis were significantly higher than our calculated frequencies (see table 3).

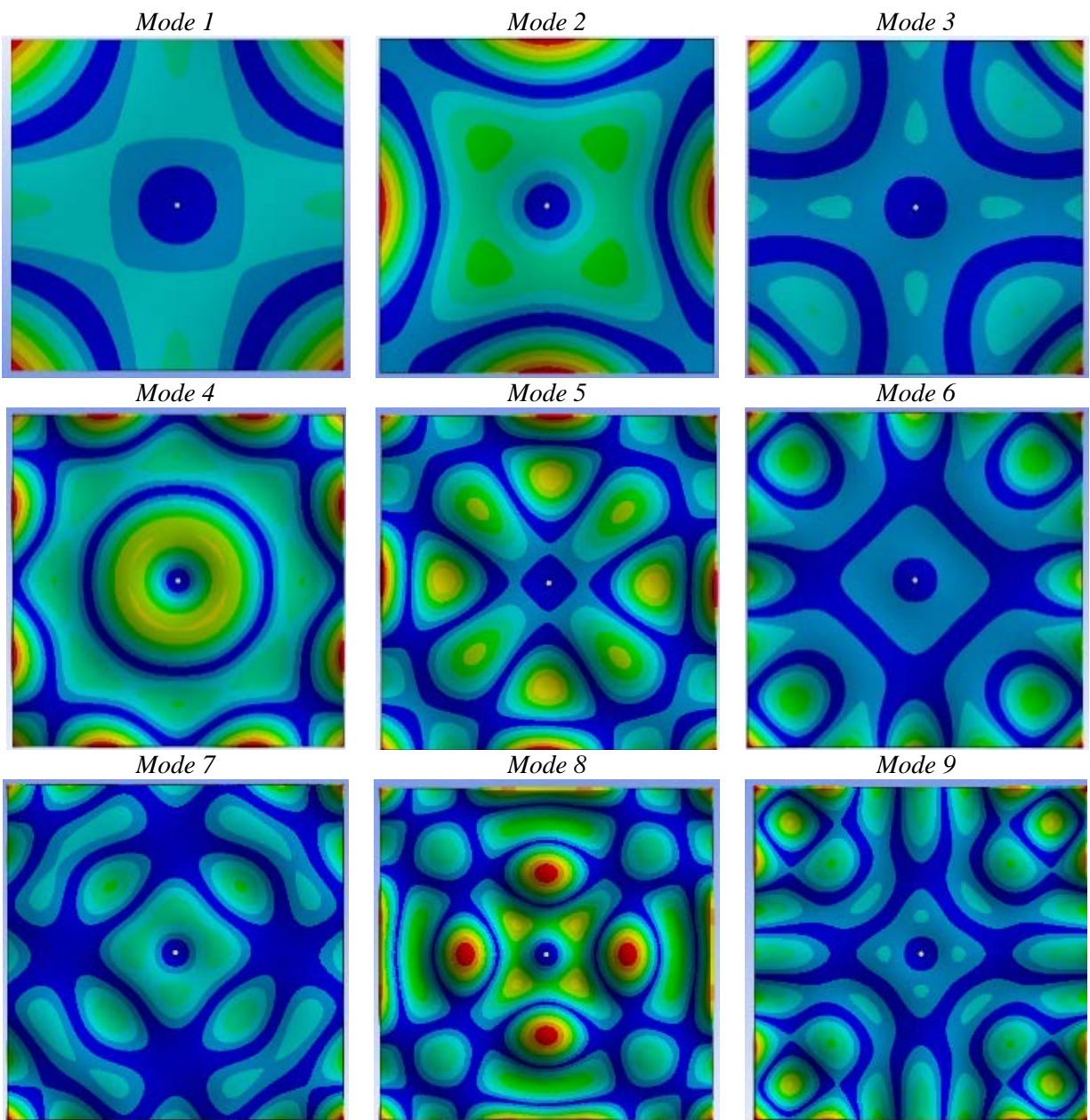


Figure 5. Visualizations of the first nine mode shapes calculated from ANSYS simulations.

Table 3. The frequencies associated with the first nine mode shapes calculated from ANSYS simulations.

	Mode 1	Mode 2	Mode 3	Mode 4	Mode 5	Mode 6	Mode 7	Mode 8	Mode 9
Calculated frequency (Hz)	237.02	456.91	731.87	1184.1	1471.4	1624.2	2135.4	2642.5	2892.7
Jiao, et al. [12] (Hz)	4685.6	8925.9	14,442	22,688	29,322	-	-	-	-

Experimental Test Results

In figure 6, pictures for each of the mode shapes are presented with their associated modal frequencies for each layer height fabricated. For some mode shapes at a given layer height, the Chladni patterns formed by the sand were not clearly distinguishable and the resulting shape varied slightly or was less pronounced. This is clearly seen for mode shapes 5, 6, and 9. For other observed mode shapes, the layer height during fabrication did not affect the formation of stable Chladni patterns. This is especially true for mode shapes 1, 2, and 4.

In table 4, the experimentally determined frequencies associated with the observed mode shapes recorded from this investigation are presented. A non-uniform relationship between layer height and mode shape is found as layer height 0.25 mm to 0.20 mm see an increase in response frequency while 0.20mm to 0.15 mm a decrease in response frequency is observed. An increase in response frequency is observed from 0.15 mm to 0.10 mm to 0.05 mm. The next observation is that the values for response frequency develop a larger variance in values as the excitation frequency increases. At each mode shape, the range in frequency can be observed in table 4 below. As the driven frequency for the system increases, the range for achieving the same mode shape between each of the five 3D printed plates grows larger. This observation is also shown graphically in figure 7 (left) which plots each plates frequency found for each respective mode shape. Figure 7 (right) plots the solution to the experimental results directly assessed with the respective frequency calculated from the finite element simulations to find the relationship. The figure plots the error between the two values against the simulated frequency to get the error value, which is represented as $0.03 = 3\%$ error.

Table 4. The observed frequencies associated with the first nine mode shapes at varying 3D printed layer heights.

Layer Height	Mode 1 (Hz)	Mode 2 (Hz)	Mode 3 (Hz)	Mode 4 (Hz)	Mode 5 (Hz)	Mode 6 (Hz)	Mode 7 (Hz)	Mode 8 (Hz)	Mode 9 (Hz)
0.25 mm	235	436	680	1102	1377	1508	1994	2465	2696
0.20 mm	250	465	726	1179	1472	1612	2128	2642	2878
0.15 mm	242	448	702	1136	1415	1560	2062	2558	2812
0.10 mm	257	482	747	1208	1506	1656	2188	2712	2972
0.05 mm	260	489	756	1226	1518	1665	2198	2730	2986
Frequency Range	25	53	76	124	141	157	204	265	290

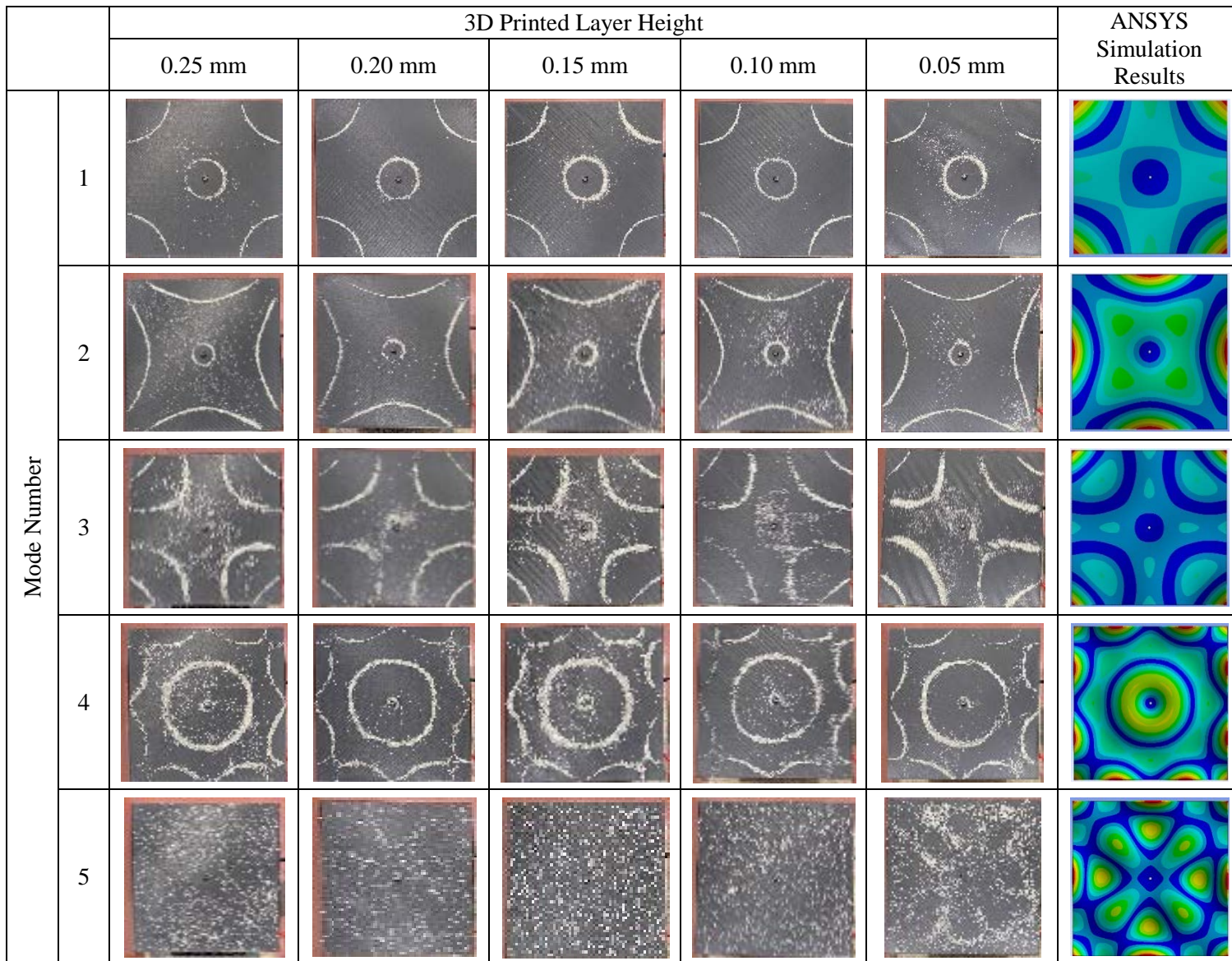


Figure 6. Visualizations of experimental observations of mode shapes compared to mode shapes obtained from ANSYS simulations.

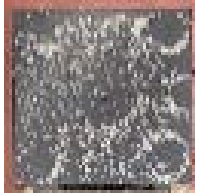




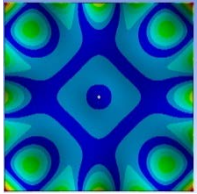
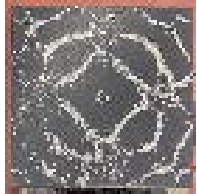




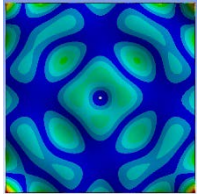





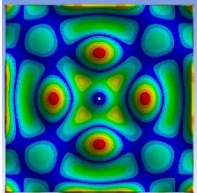



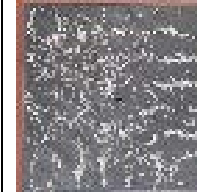

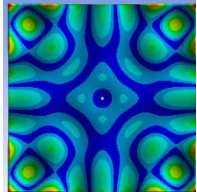
		3D Printed Layer Height					ANSYS Simulation Results
		0.25 mm	0.20 mm	0.15 mm	0.10 mm	0.05 mm	
Mode Number	6						
	7						
	8						
	9						

Figure 6 (continued). Visualizations of experimental observations of mode shapes compared to mode shapes obtained from ANSYS simulations.

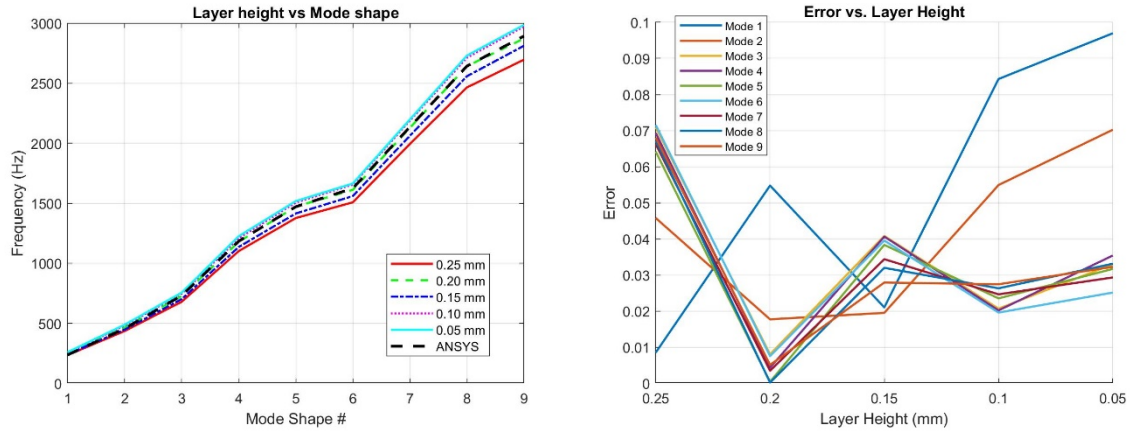


Figure 7. Frequencies vs. layer height (left) and error vs. layer height for modes 1-9 (right).

Conclusions

As continued investigations focus on the mechanical properties of 3D printed materials, a critical understanding of the modal characteristics of these materials will play an increasingly bigger role in mechanical performance considerations. In this investigation, it was found for PLA that the layer height significantly affects vibrational response in the medium. The experimental results were compared to ANSYS finite element analysis simulations of a pure PLA Chladni plate system with FFFF boundary conditions. A convergence towards a 3% error was observed with increasing frequency mode shapes. For design considerations, these experimental observations suggest that when dealing with a lower frequency mode shape made from 3D-printed materials layer height is not a critical factor. As the frequency increases, the importance of layer height becomes an increasingly important factor to consider. Further investigation into this topic is necessary to continue to develop a deeper understanding of the modal characteristics of 3D printed materials and their importance in the mechanical nature of design.

References

- [1] H. El Fazani, E. Austen, and J. Laliberte, “Effect of Infill Density on the Mechanical Properties of Additive Manufactured Parts Made from PLA,” presented at the CASI AERO 21 Conference, Online: Canadian Aeronautics and Space Institute, Jun. 2021, pp. 1–13. Accessed: Apr. 12, 2024. [Online]. Available: <https://casi.ca/resources/Documents/AERO/2021/Full%20Papers/Effect%20of%20Infill%20Density%20on%20the%20Mechanical%20Properties%20of%20Additive%20Manufactured%20Parts%20Made%20from%20PLA.docx>
- [2] D. Frunzaverde *et al.*, “The Influence of the Layer Height and the Filament Color on the Dimensional Accuracy and the Tensile Strength of FDM-Printed PLA Specimens,” *Polymers*, vol. 15, no. 10, p. 2377, May 2023, doi: 10.3390/polym15102377.
- [3] J. R. Stojković *et al.*, “An Experimental Study on the Impact of Layer Height and Annealing Parameters on the Tensile Strength and Dimensional Accuracy of FDM 3D Printed Parts,” *Materials*, vol. 16, no. 13, p. 4574, Jun. 2023, doi: 10.3390/ma16134574.
- [4] H. T. Nguyen, K. Crittenden, L. Weiss, and H. Bardaweel, “Experimental Modal Analysis and Characterization of Additively Manufactured Polymers,” *Polymers*, vol. 14, no. 10, p. 2071, May 2022, doi: 10.3390/polym14102071.
- [5] F. He, H. Ning, and M. Khan, “Effect of 3D Printing Process Parameters on Damping Characteristic of Cantilever Beams Fabricated Using Material Extrusion,” *Polymers*, vol. 15, no. 2, p. 257, Jan. 2023, doi: 10.3390/polym15020257.
- [6] F. Medel, J. Abad, and V. Esteban, “Stiffness and damping behavior of 3D printed specimens,” *Polymer Testing*, vol. 109, p. 107529, May 2022, doi: 10.1016/j.polymertesting.2022.107529.
- [7] E. Abdeddine, A. Majid, Z. Beidouri, and K. Zarbane, “Experimental investigation for non-linear vibrations of free supported and cantilever FFF rectangular plates,” *Archives of Materials Science and Engineering*, vol. 116, no. 2, pp. 49–56, Aug. 2022, doi: 10.5604/01.3001.0016.1189.
- [8] T. D. Rossing, “Chladni’s law for vibrating plates,” *American Journal of Physics*, vol. 50, no. 3, pp. 271–274, Mar. 1982, doi: 10.1119/1.12866.
- [9] T. D. Rossing and D. A. Russell, “Laboratory observation of elastic waves in solids,” *American Journal of Physics*, vol. 58, no. 12, pp. 1153–1162, Dec. 1990, doi: 10.1119/1.16245.
- [10] Y. Song, Y. Li, W. Song, K. Yee, K.-Y. Lee, and V. L. Tagarielli, “Measurements of the mechanical response of unidirectional 3D-printed PLA,” *Materials & Design*, vol. 123, pp. 154–164, Jun. 2017, doi: 10.1016/j.matdes.2017.03.051.

- [11] J. Prusa, "Layers and perimeters," Prusa Knowledge Base. Accessed: Aug. 28, 2024. [Online]. Available: https://help.prusa3d.com/article/layers-and-perimeters_1748
- [12] X. Jiao, J. Tao, H. Sun, and Q. Sun, "Modeling of Acoustic Vibration Theory Based on a Micro Thin Plate System and Its Control Experiment Verification," *Sustainability*, vol. 14, no. 22, p. 14900, Nov. 2022, doi: 10.3390/su142214900.